SAND2016-11933PE

Exceptional service in the national interest

Sandia National Laboratories

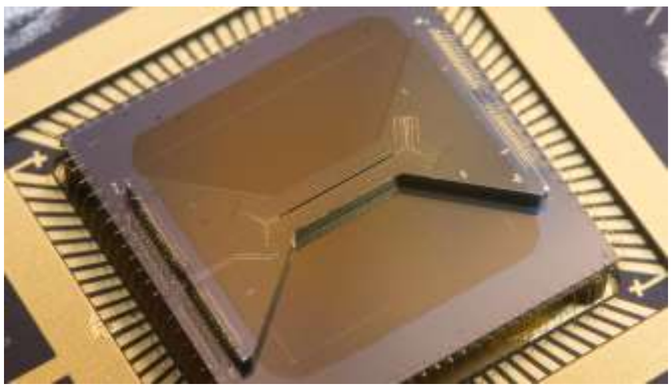

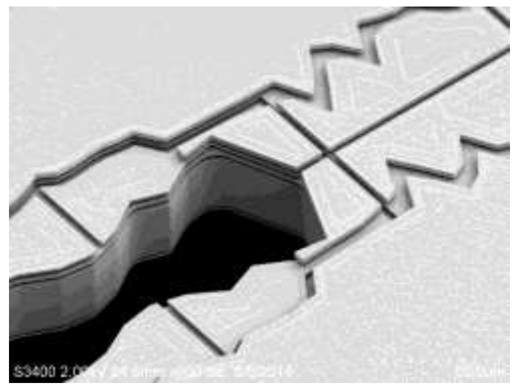

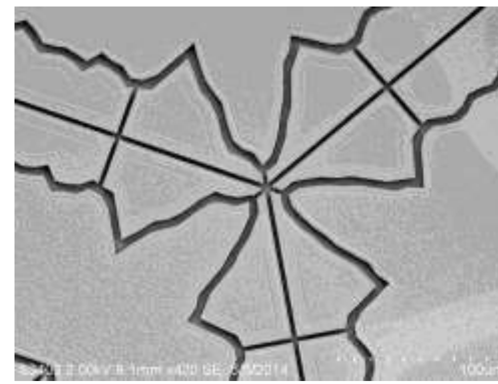

Surface ion traps for quantum computing

Optics and Quantum Electronics Seminar (October 12, 2016)

Dr. Daniel Stick

U.S. DEPARTMENT OF ENERGY

NNSA National Nuclear Security Administration

Sandia National Laboratories

Outline

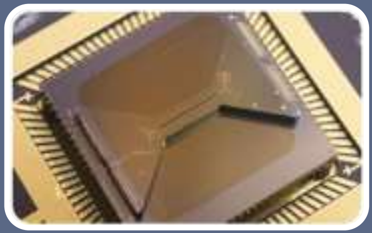

Trap features

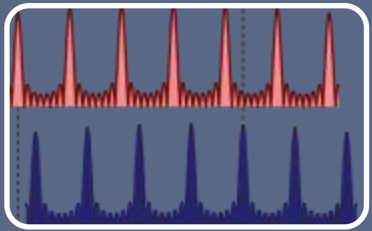

Experimental characterization

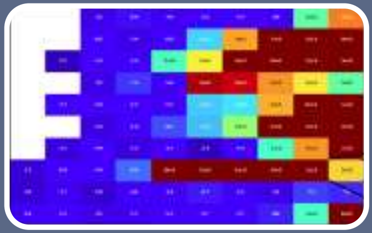

Single qubit gates

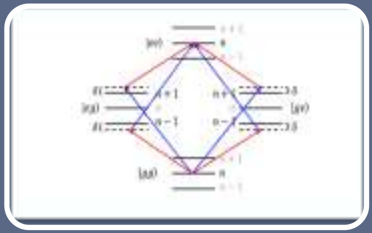

Mølmer-Sørensen two-qubit gate

Advantages/Challenges vs 3D

Advantages

- More manufacturable ("scalable")
- Consistent geometry -> consistent behavior
- Greater field control (more electrodes)
- 2D geometry
- Integration of other technologies (waveguides, detectors, filters…)
- Laser access

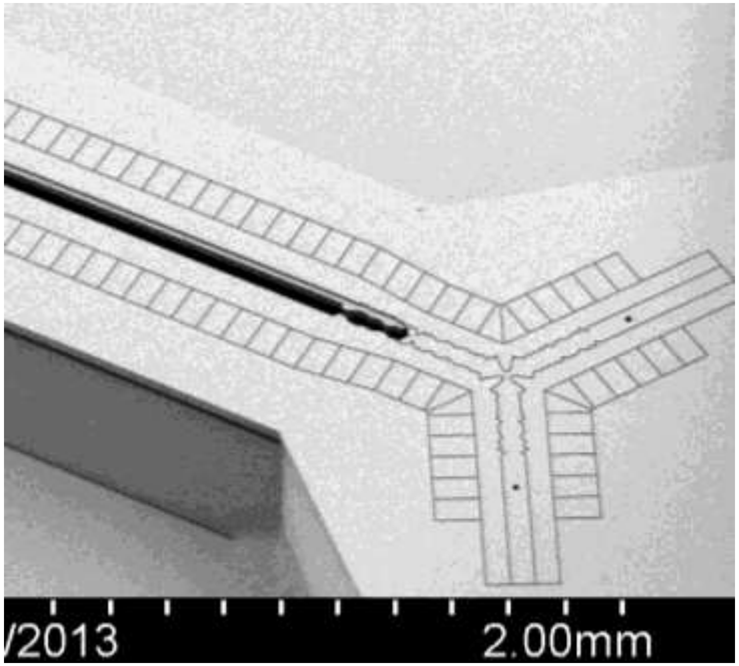

Challenges

- Low depth (ion lifetime), anharmonicities in potential
- Proximity to surface (charging, heating)
- Delicate (dust, voltage)
- Capacitance

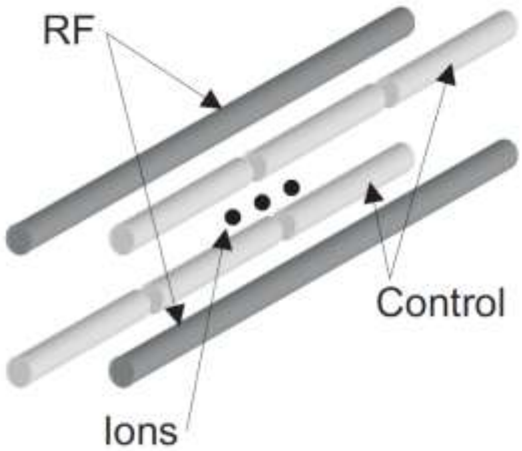

Capabilities & Requirements

Essential capabilities

- Store ions for long periods of time (hours)
- Move ions to achieve 2D connectivity
- Support high fidelity operations
- Uniform performance

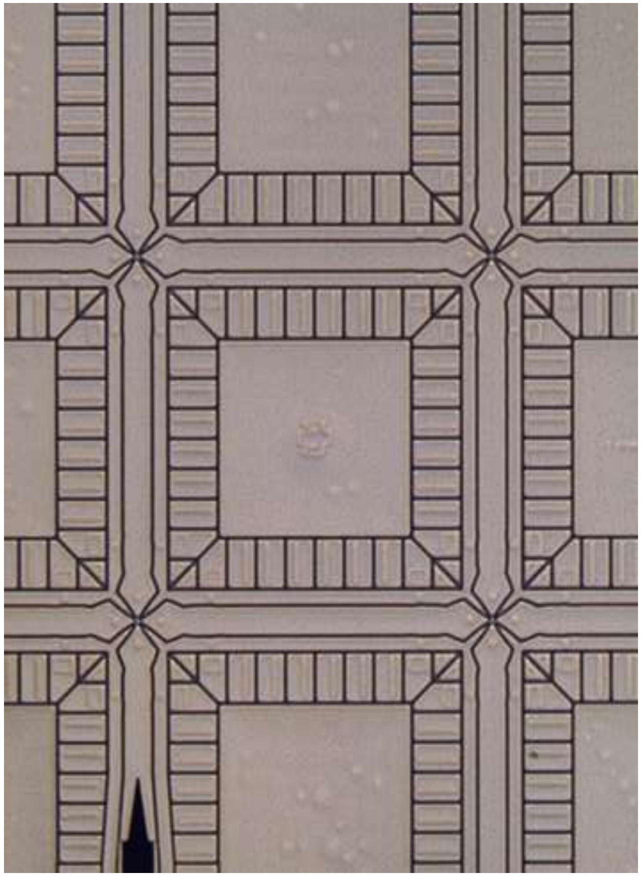

Derived requirements

- Voltage breakdown >300 V @ ~50 MHz
- Backside loading hole
- Multi-level lead routing for accessing interior electrodes
- Standardization [lithographically defined electrodes]
- Overhung electrodes
- High optical access [high NA delivery and collection optics]

Voltage application

Trapping potential

- Axial frequency: 500 kHz [<5 V]
- Radial frequency: 2.8 MHz, 3.1 MHz [250 Vrf @ 40 MHz]

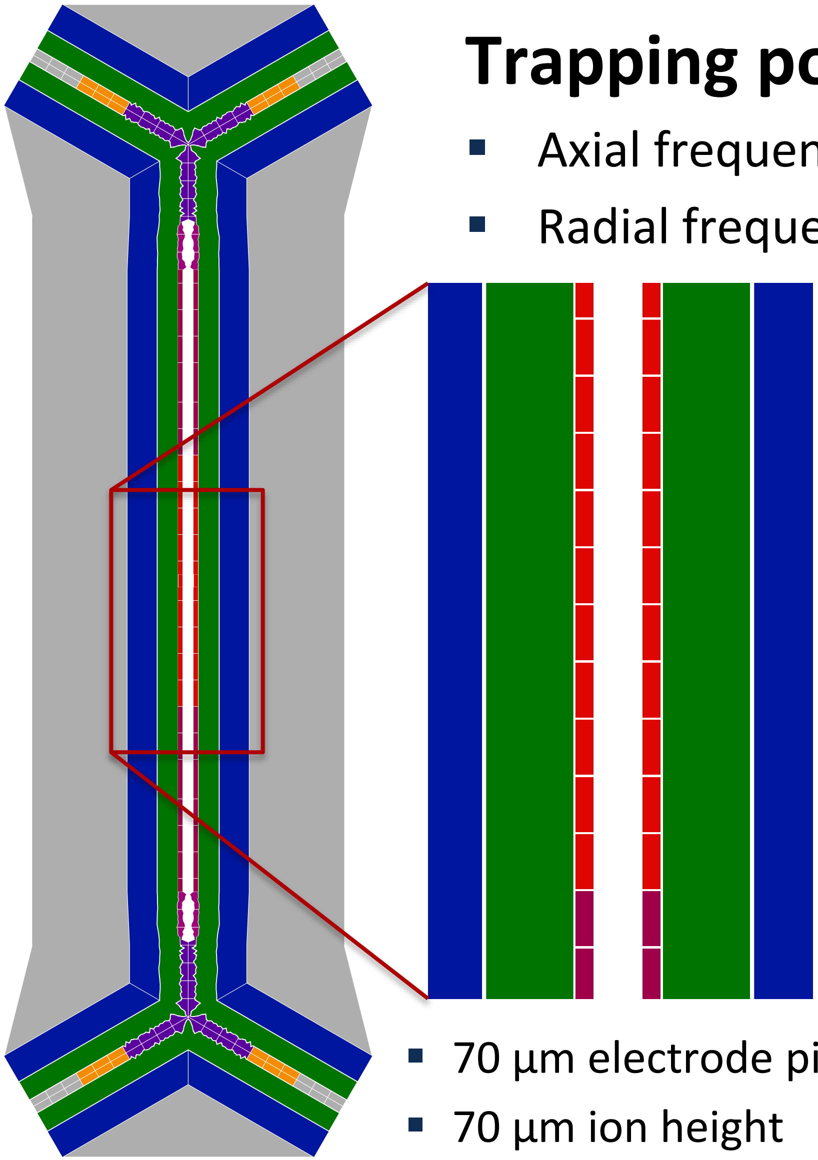

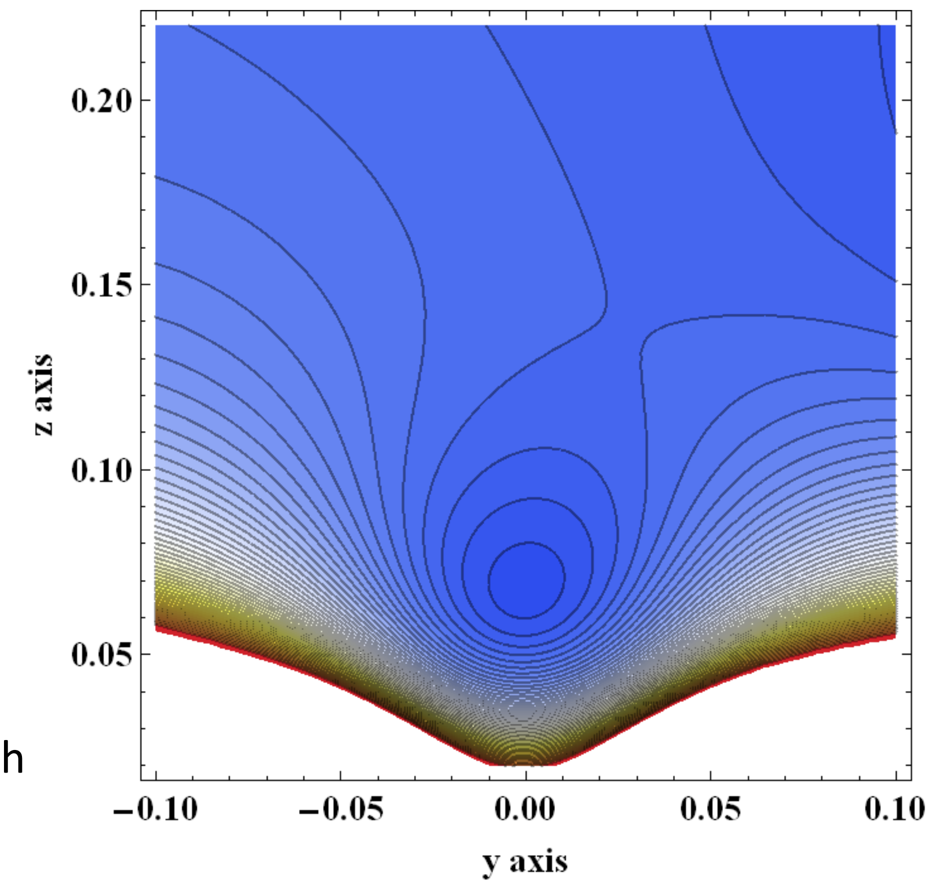

- 70 µm electrode pitch
- 70 µm ion height

Multi-layer metallization

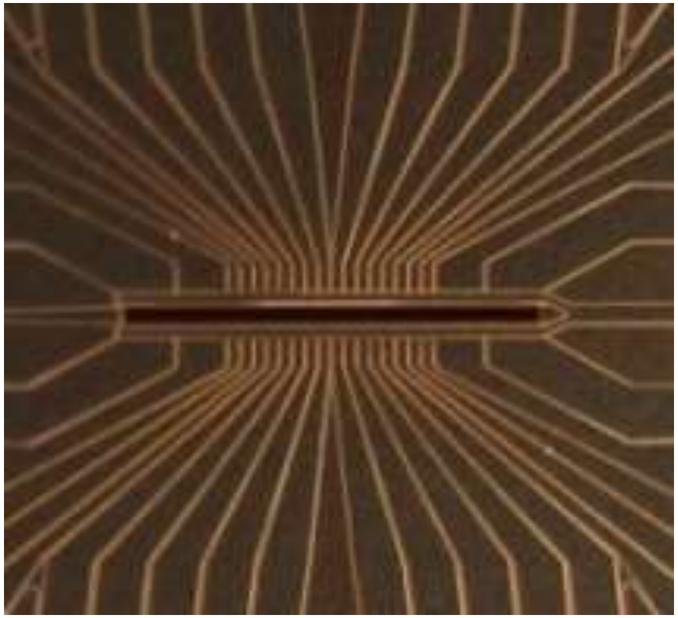

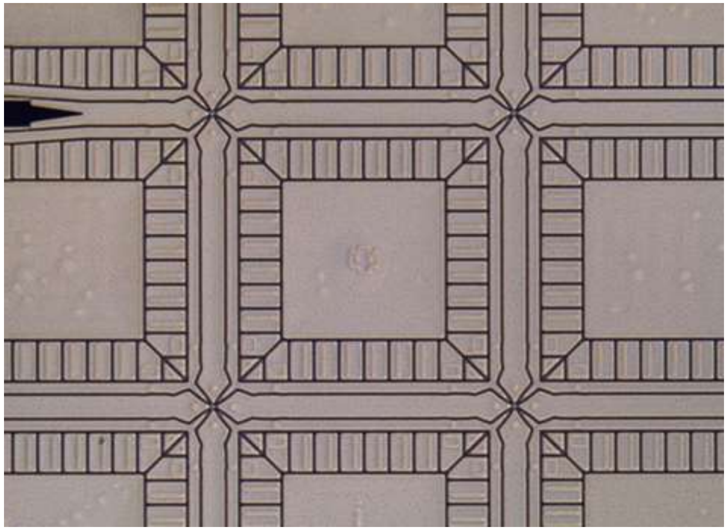

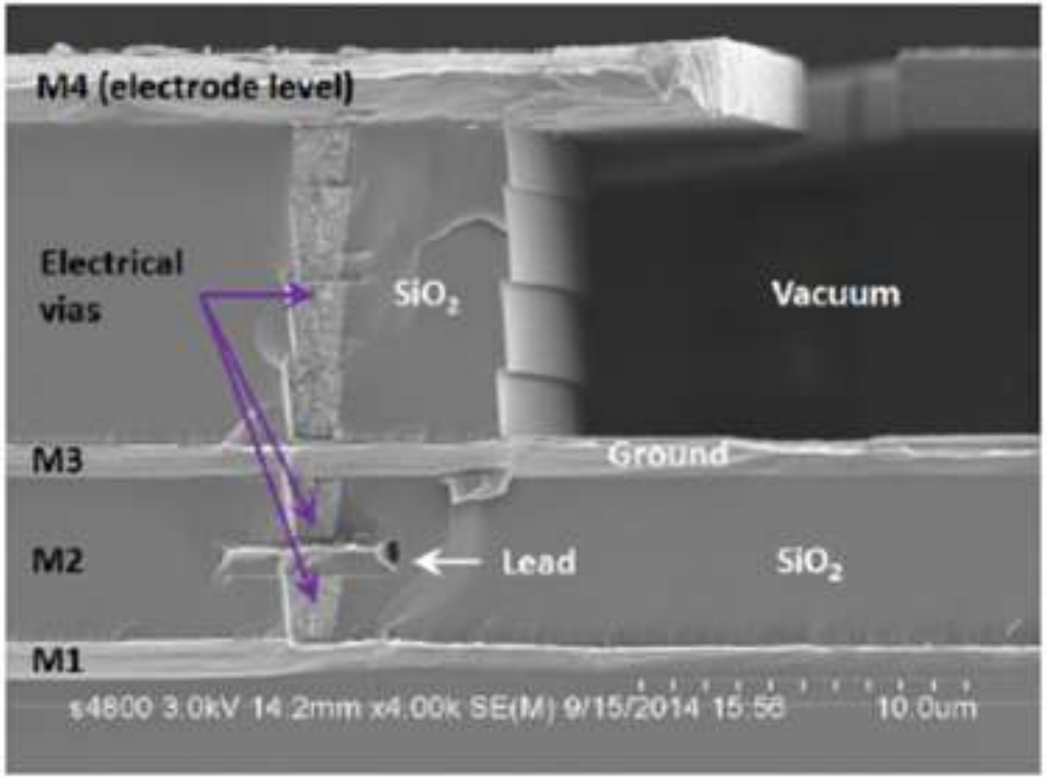

Trench capacitors & Loading holes

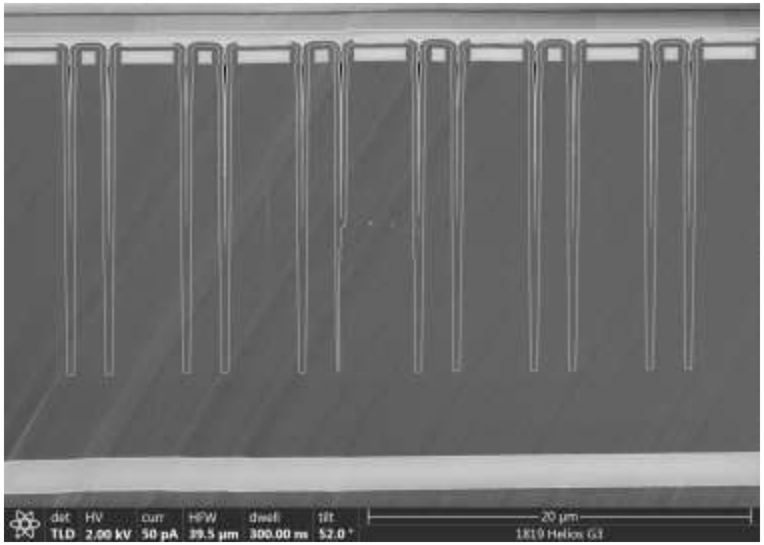

Interposer (current)

- 20V max voltage
- 1nF capacitance

On chip (future)

- 15V max voltage
- 200pF capacitance (but low inductance)
- Up to 200 capacitors can be located within the isthmus

50µm×80µm
modulation necessary

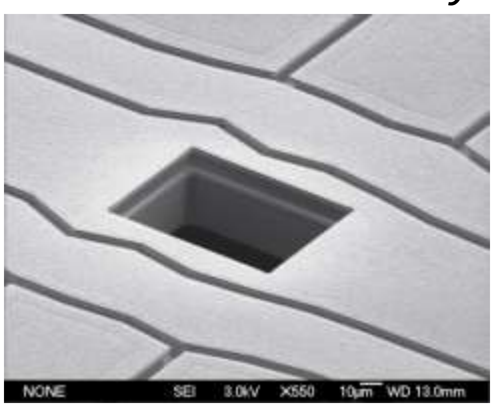

10µm hole
still perturbs the field

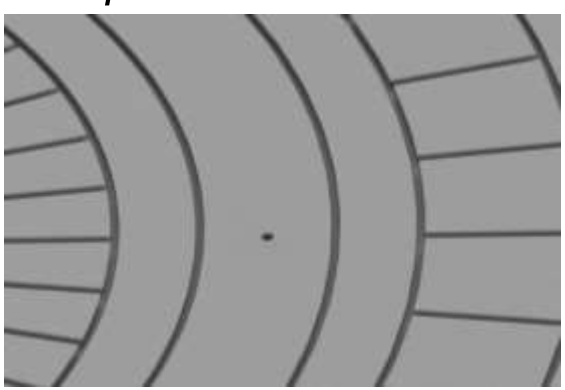

3µm×20µm

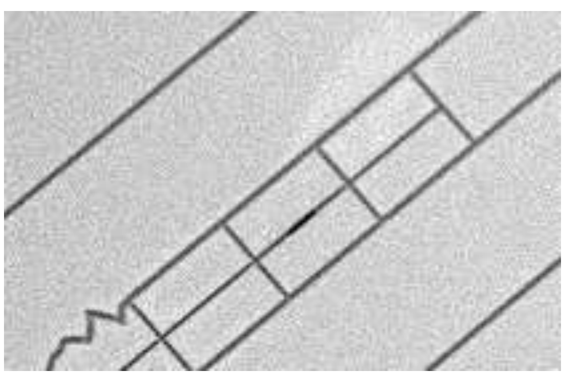

Trap features

Optical access & integrated optics

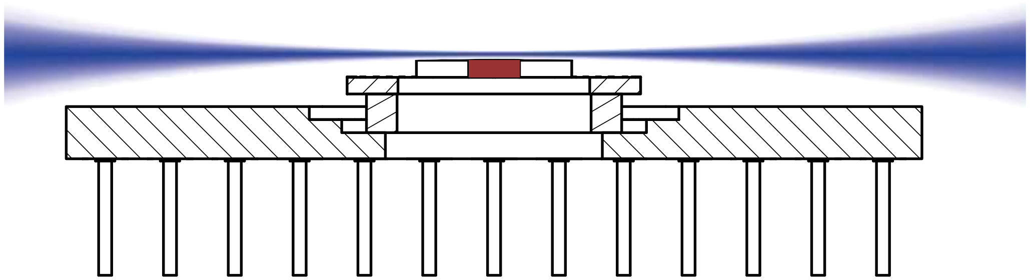

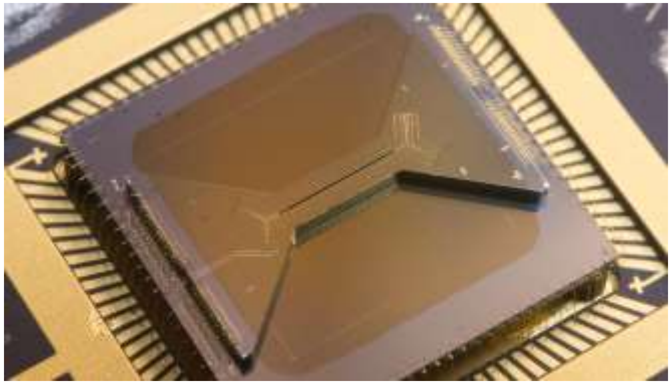

Can accommodate 4/2 um beam waist (369 nm)

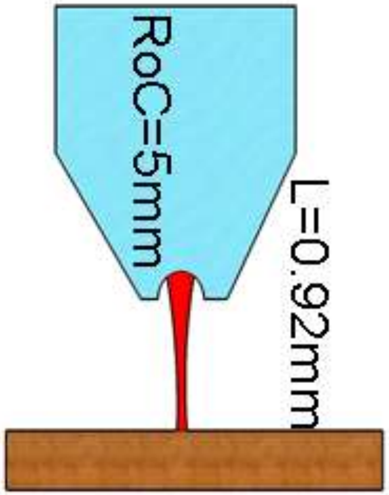

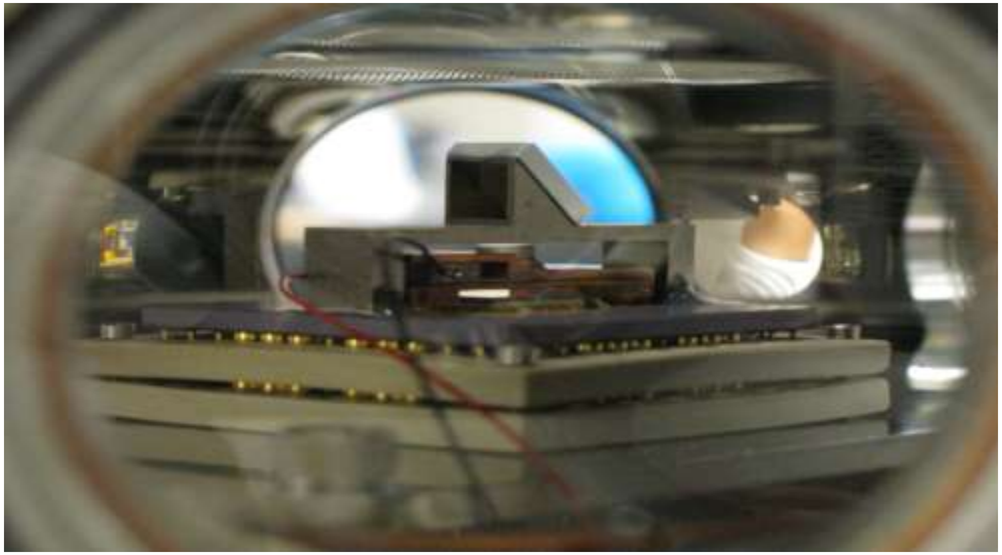

Trap features

Manufacturability, uniformity

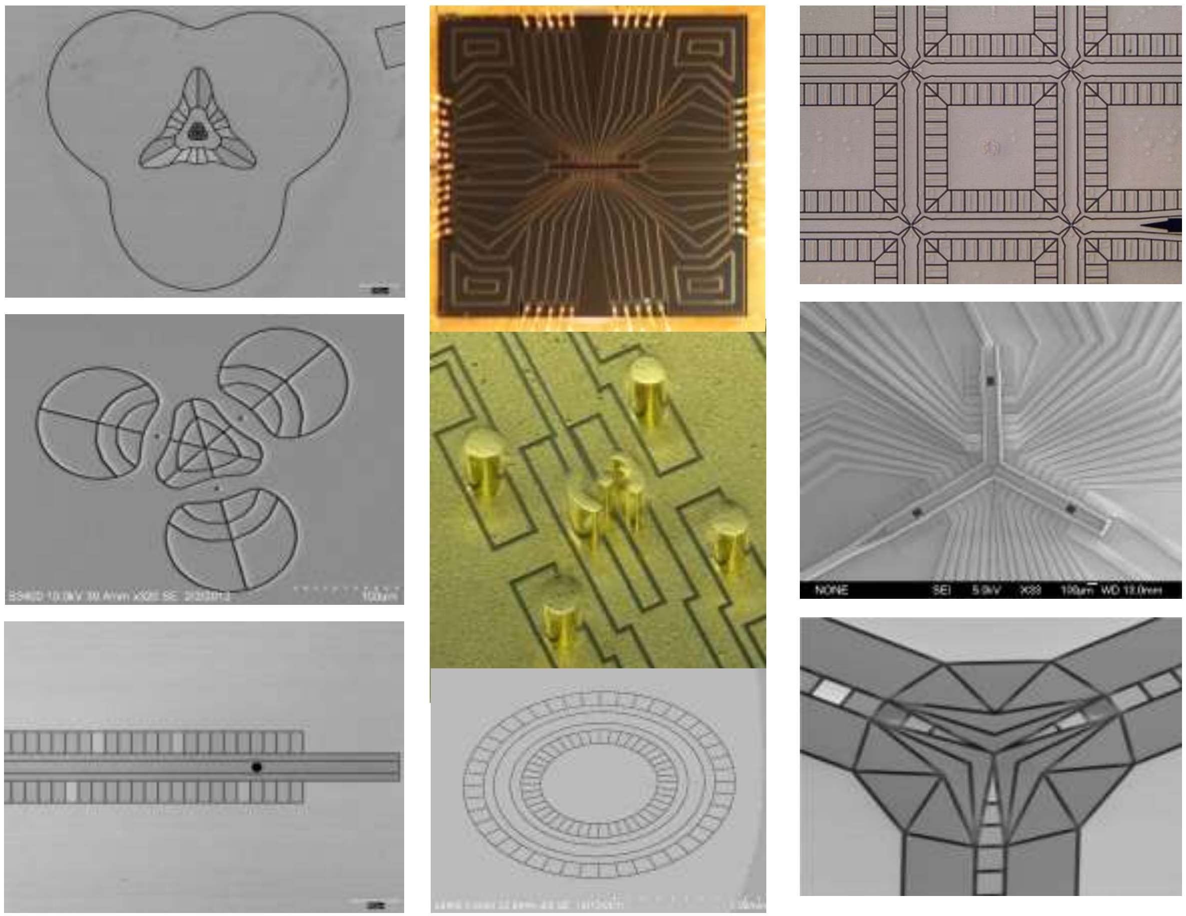

- 12 institutions, 5 countries
- >100 devices delivered
- Quantum computing
- Quantum simulations
- Quantum communication
- Surface science
- Metrology

Experimental characterization

Heating

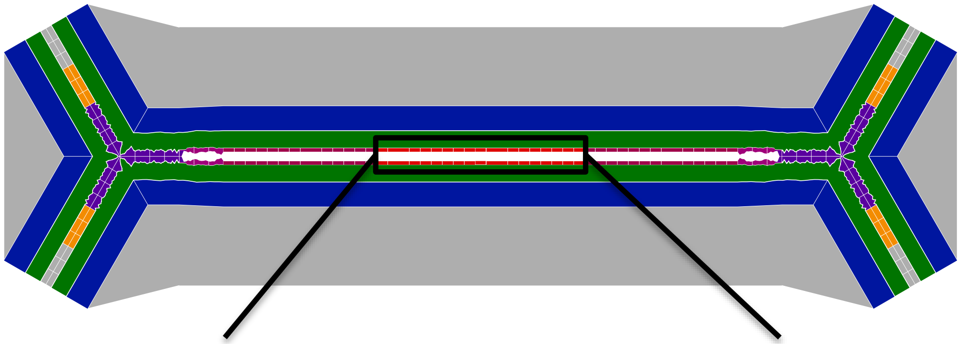

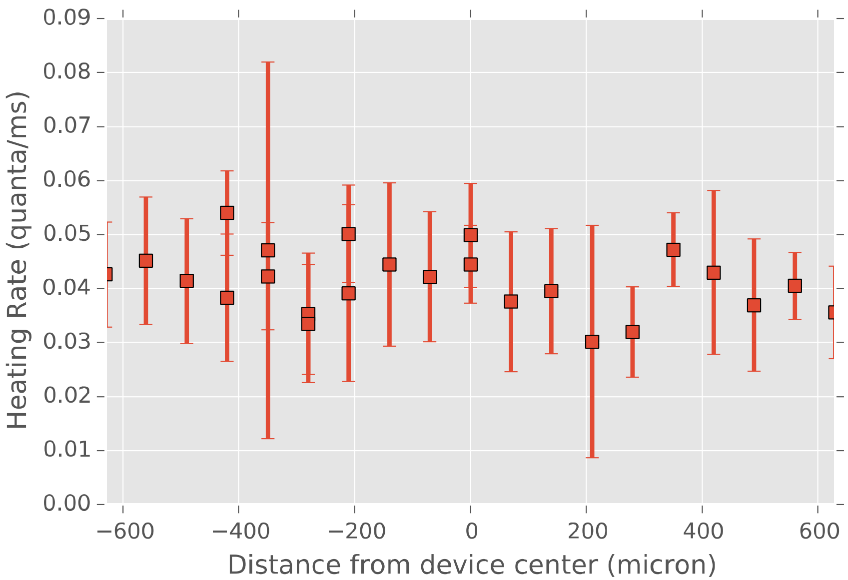

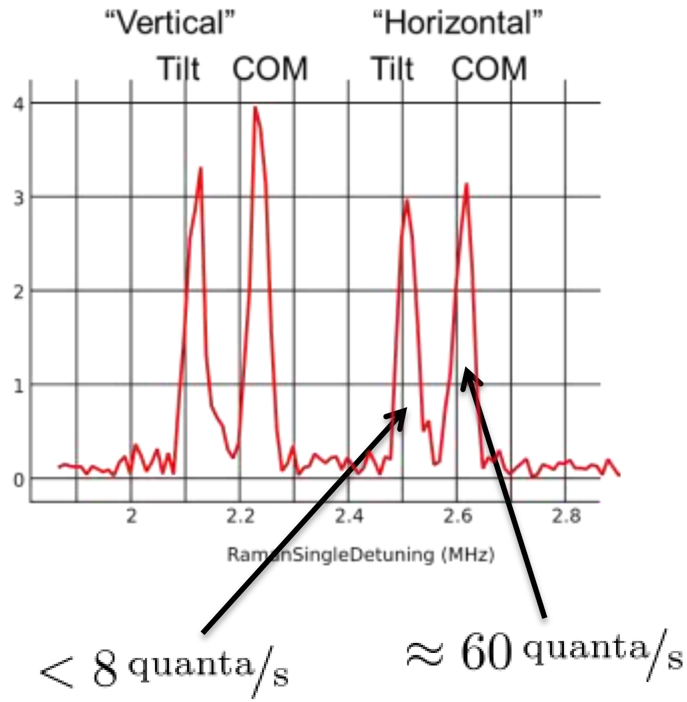

- Heating rate 40 q/s on average, $^{171}Yb^{+}$, Trap frequency 2.8 MHz, RF drive at 50 MHz
- Heating rate in HOA-2 is low and uniform along the length of the quantum section

Experimental characterization

Background electric field

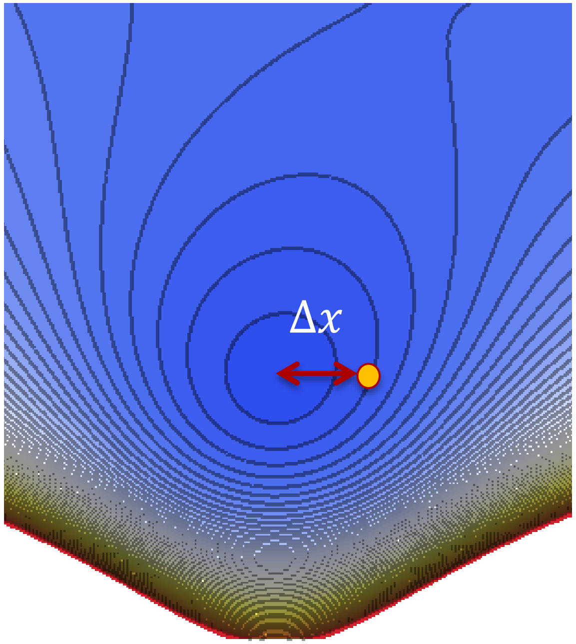

- Goal is to eliminate offset from RF null

$$x(t) = [A\cos(\omega t) + \Delta x](1 + \frac{q}{2}\cos(\Omega t))$$

- Measure transition strength of Raman beams applied at drive frequency (lateral direction)
- Tickle ion motion with chirped pulses at drive frequency, minimize fluorescence

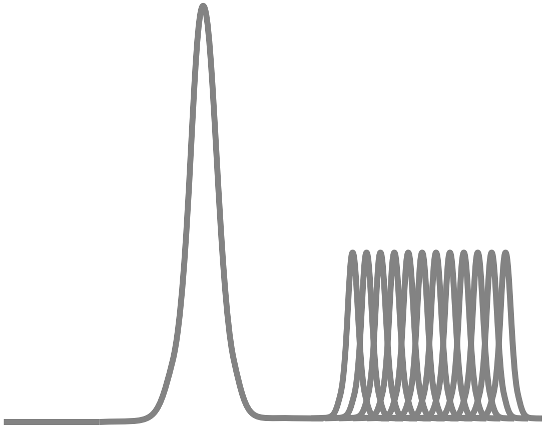

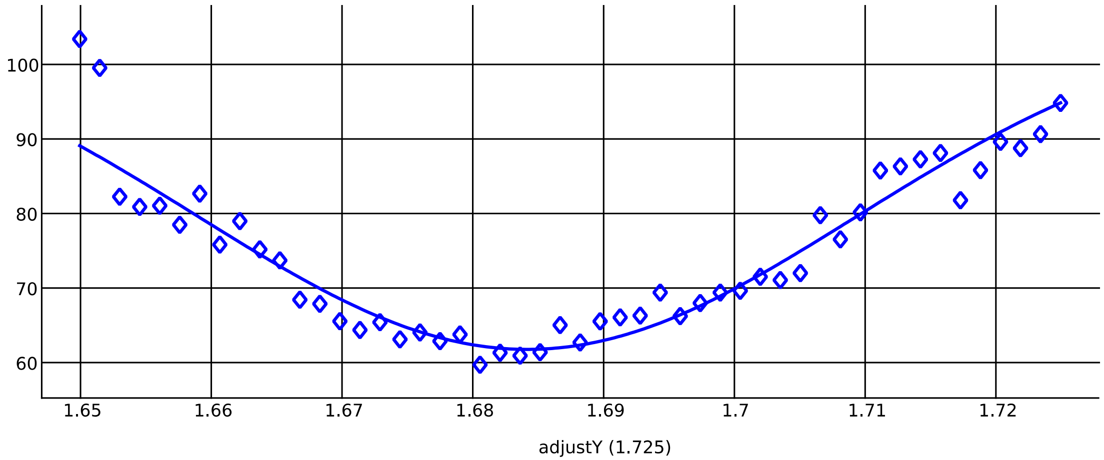

Experimental characterization

Background electric field

Linear trap

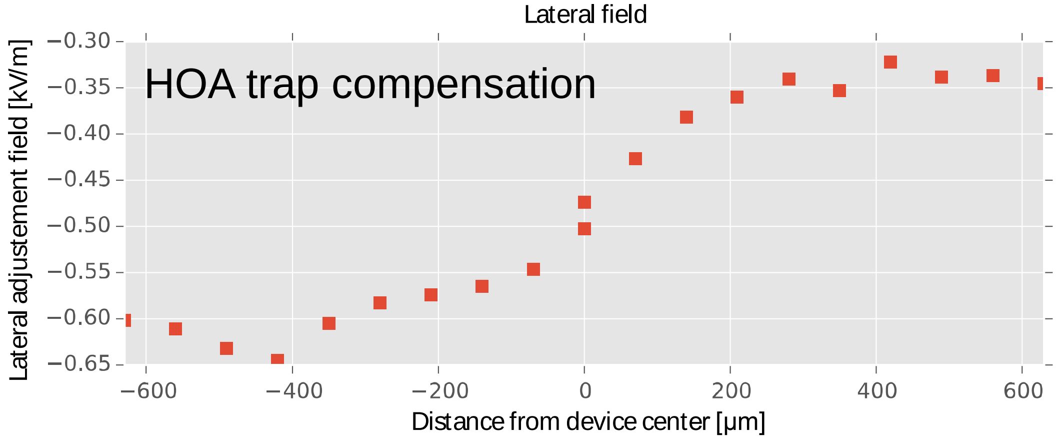

Ring trap

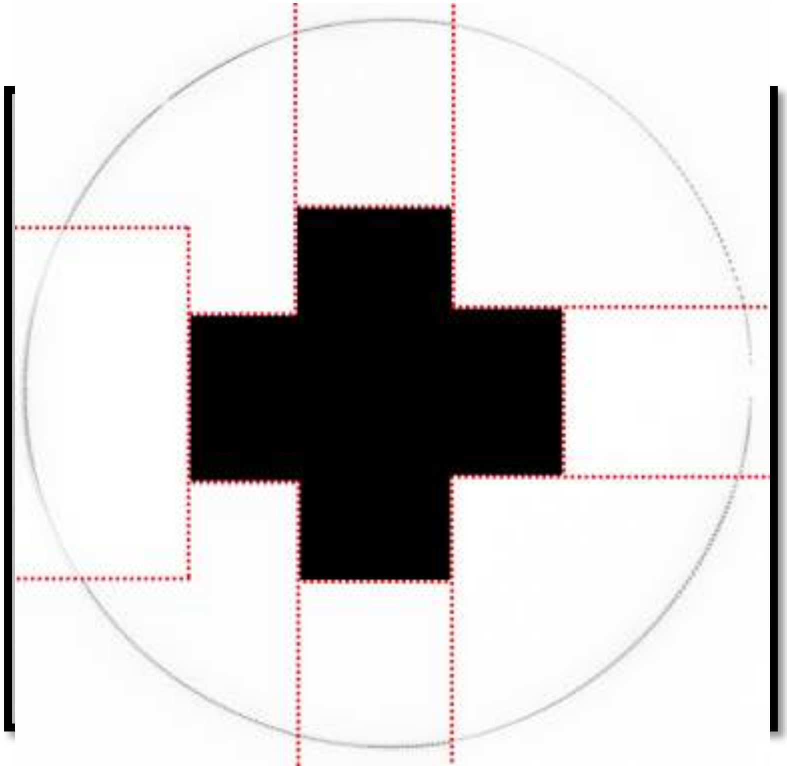

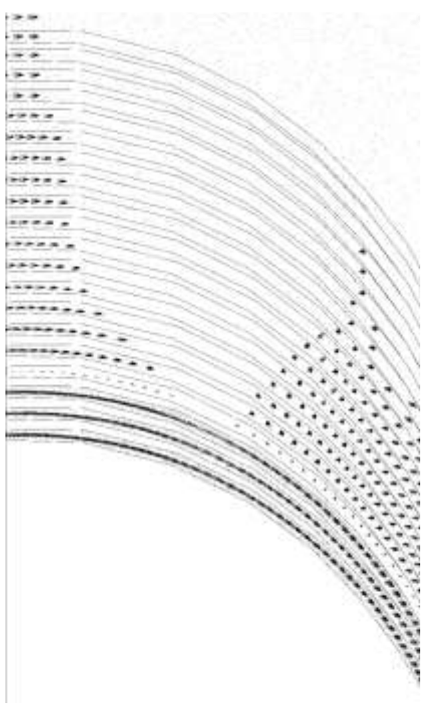

Experimental characterization

Shuttling and swapping

- Co-wired junction and linear sections, transported ions around device
- Same voltage solution at junctions

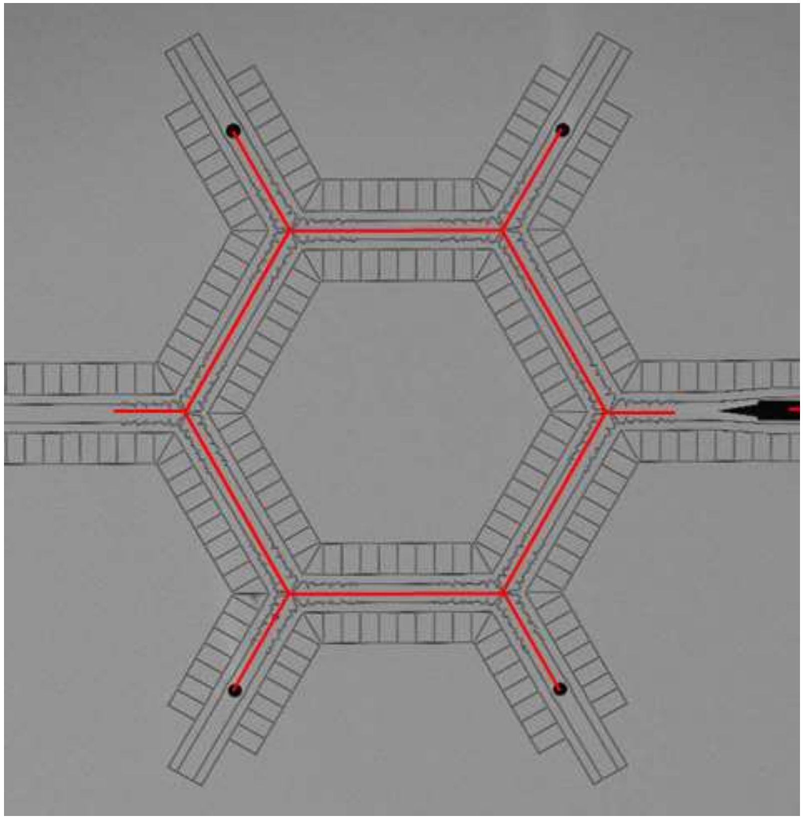

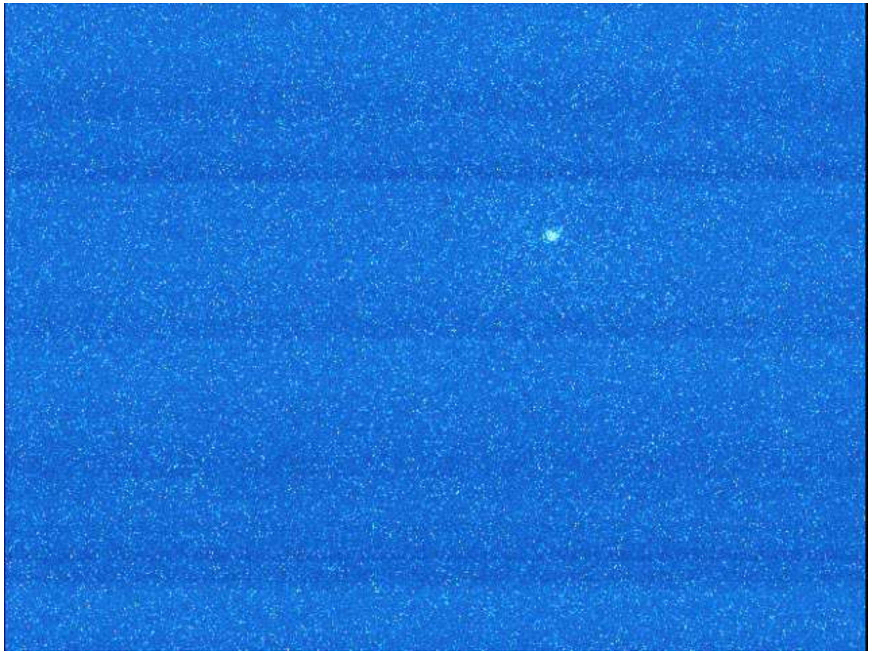

Experimental characterization

Shuttling and swapping

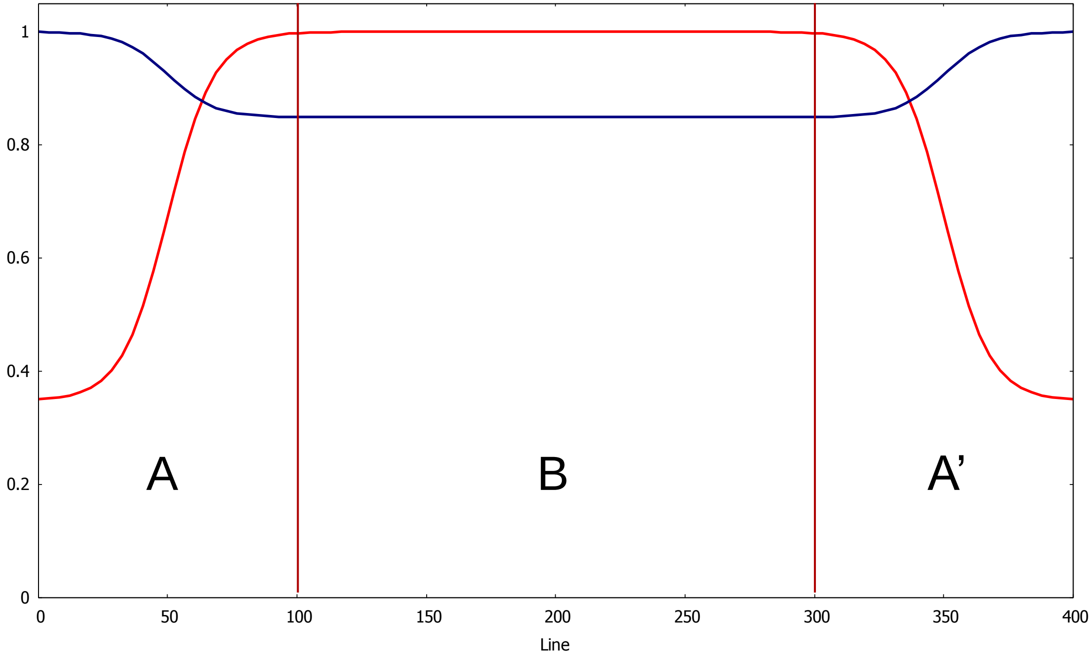

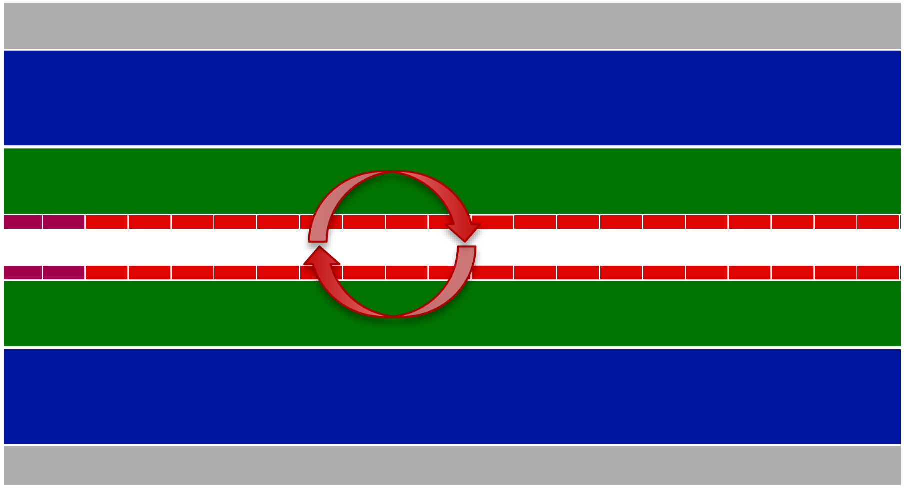

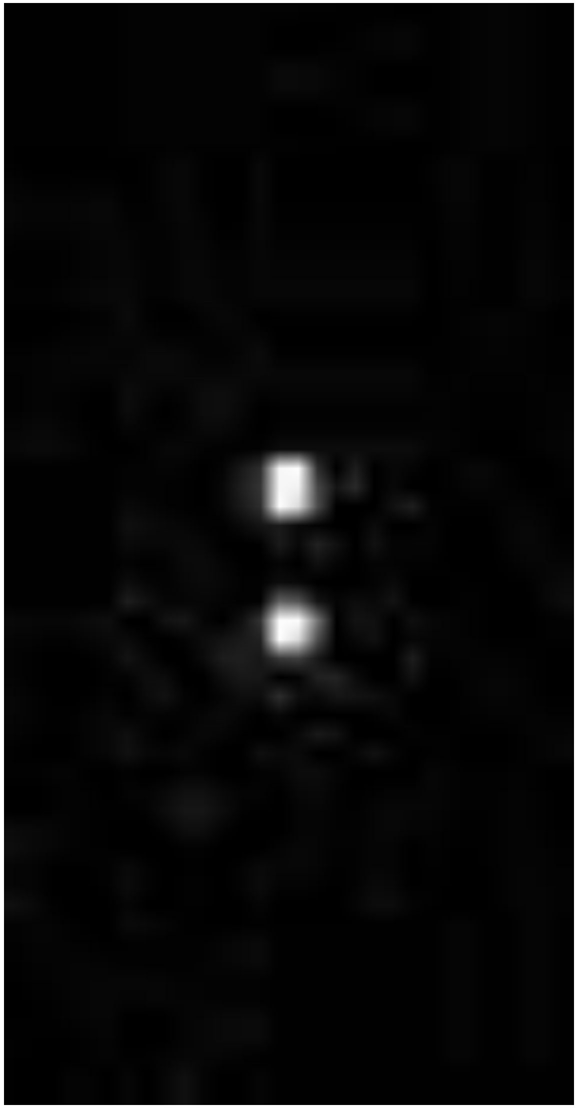

Experimental characterization

Shuttling and swapping

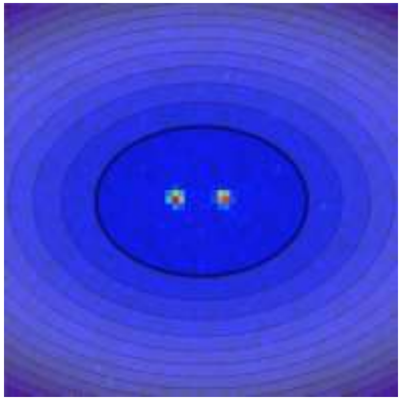

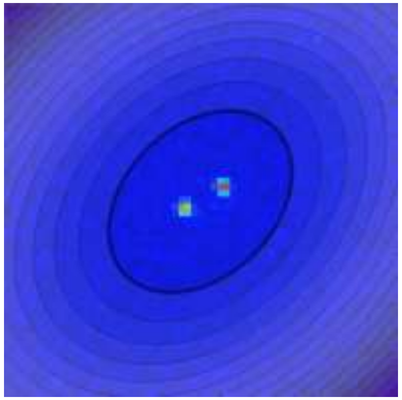

- Tag one ion with BB1 composite pulse
- Measure states on separate PMT's after rotation
  - In addition to declining success probability, fluorescence drops due to motional heating
  - Success probability drops for times <18.6 us

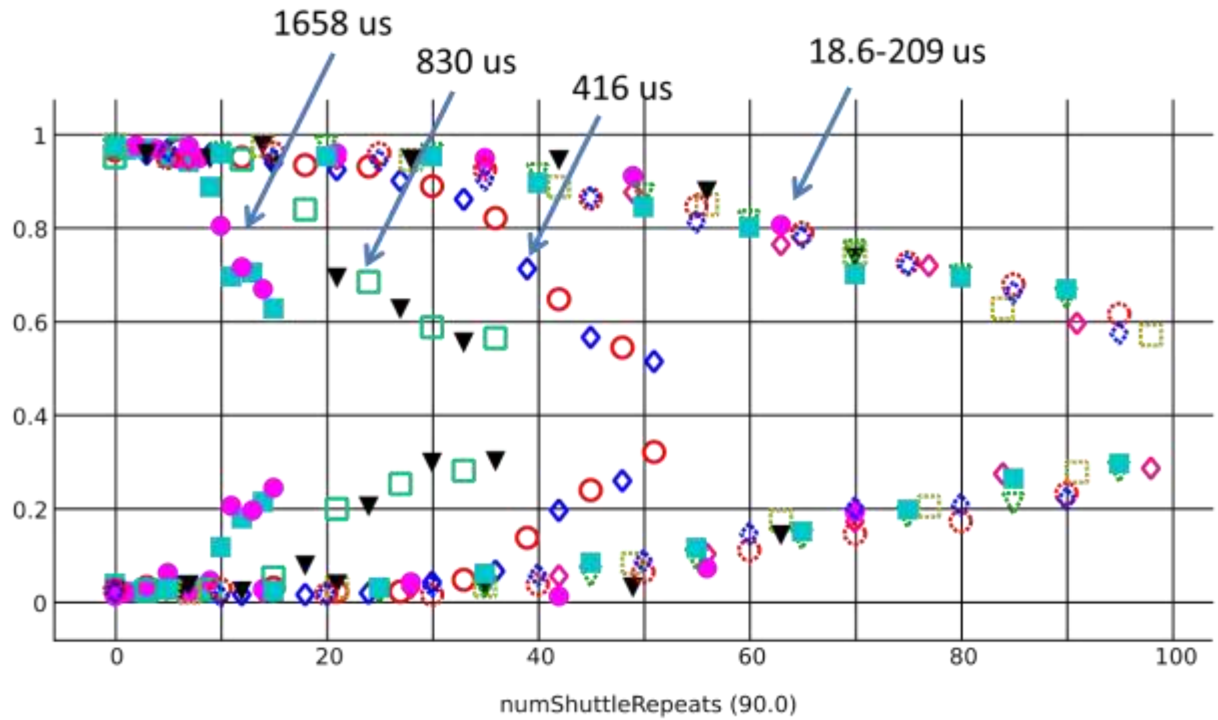

Ytterbium qubit

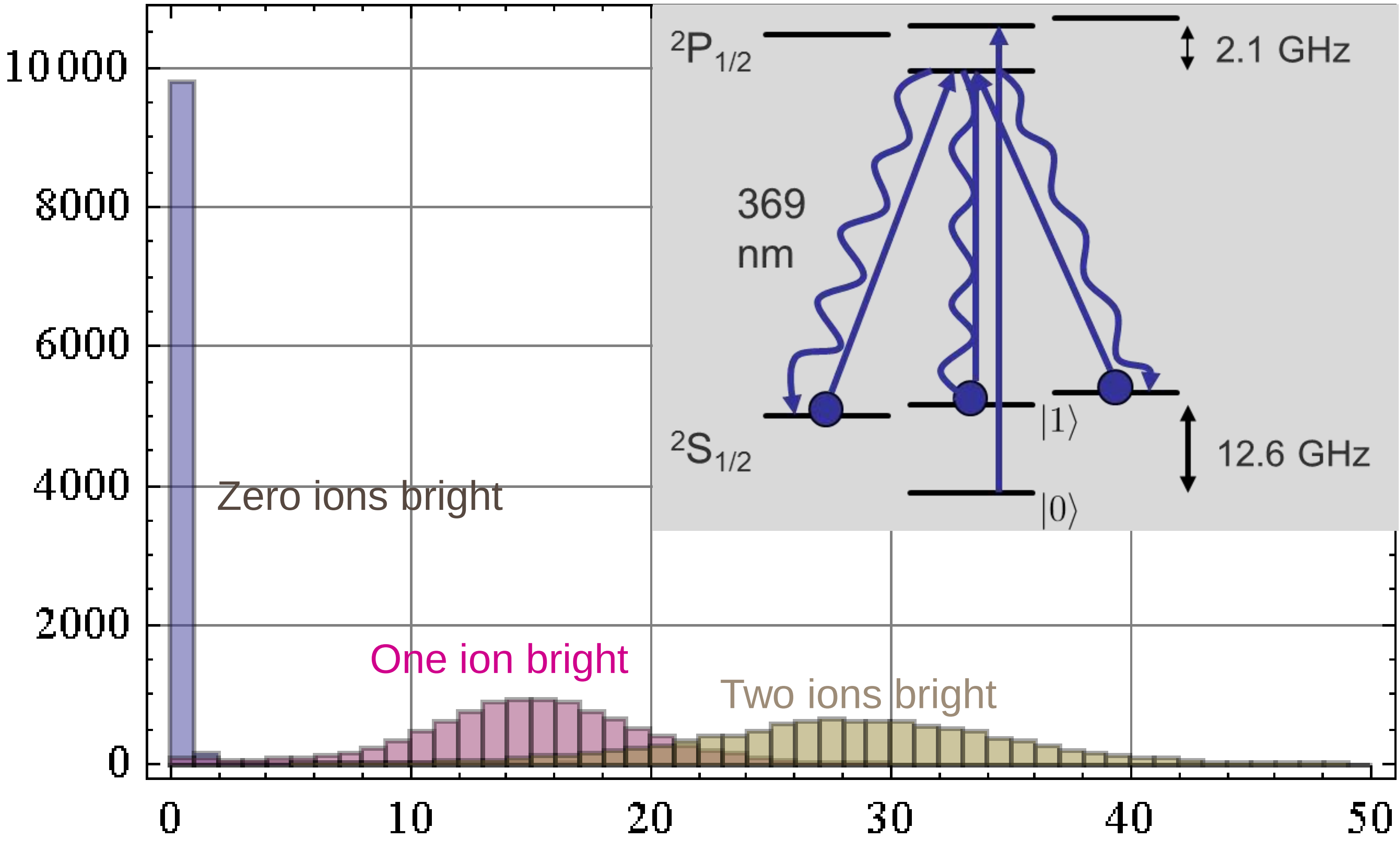

S. Olmschenk *et al.*, PRA **76**, 052314 (2007)

Sandia National Laboratories

Ytterbium qubit

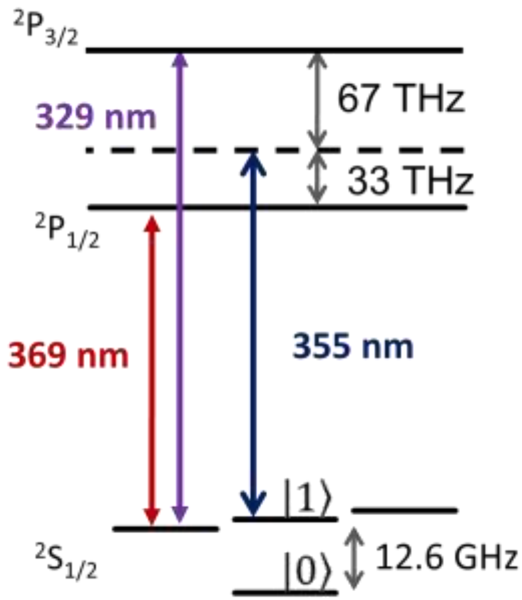

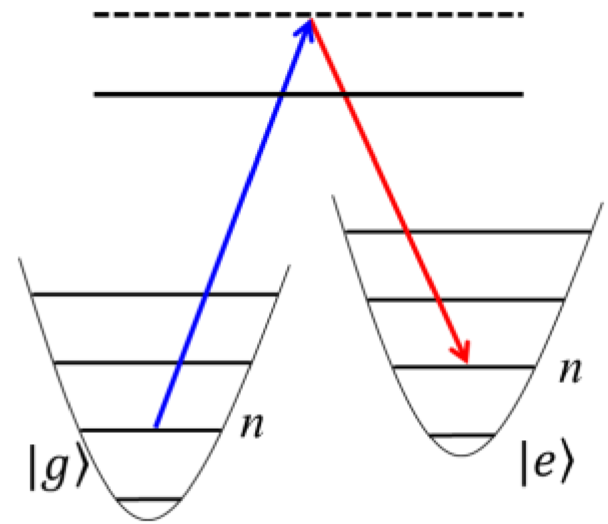

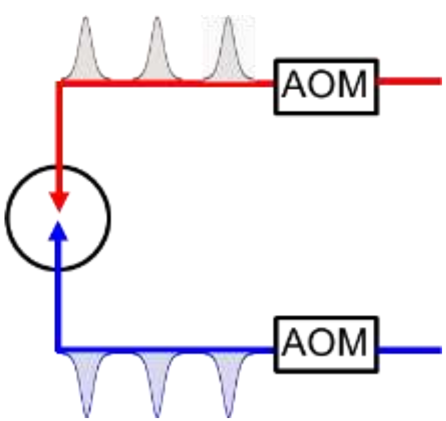

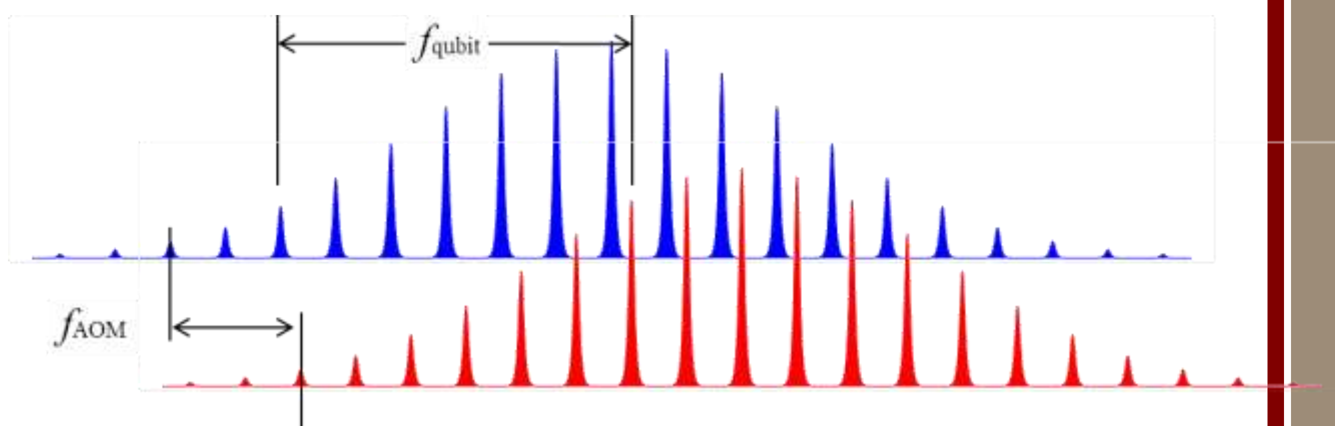

Gate Set Tomography (GST)

Desired "target" gates:

G_i	Idle (Identity)
G_x	$\pi/2$ rotation about x-axis
G_y	$\pi/2$ rotation about y-axis

- No calibration required
- Detailed debug information
- Efficiently measures performance characterizing fault-tolerance (diamond norm)
- Amplifies errors
- Detects non-Markovian noise
- Robin Blume-Kohout, SNL

Fiducials:

$\{\}$

Gx

Gy

$Gx \cdot Gx$

$Gx \cdot Gx \cdot Gx$

$Gy \cdot Gy \cdot Gy$

Germs:

Gx

Gy

Gi

$Gx \cdot Gy$

$Gx \cdot Gy \cdot Gi$

$Gx \cdot Gi \cdot Gy$

$Gx \cdot Gi \cdot Gi$

$Gy \cdot Gi \cdot Gi$

$Gx \cdot Gx \cdot Gi \cdot Gy$

$Gx \cdot Gy \cdot Gy \cdot Gi$

$Gx \cdot Gx \cdot Gy \cdot Gx \cdot Gy \cdot Gy$

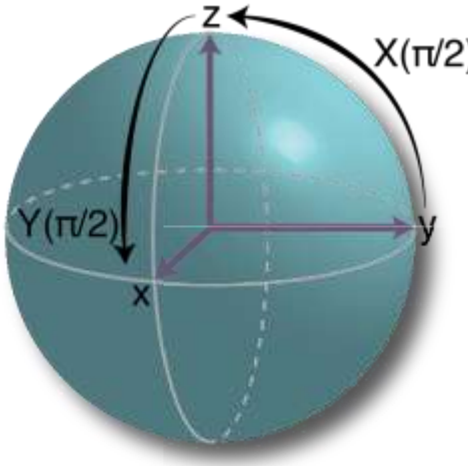

Single qubit BB1 compensated microwave gates on $^{171}Yb^+$

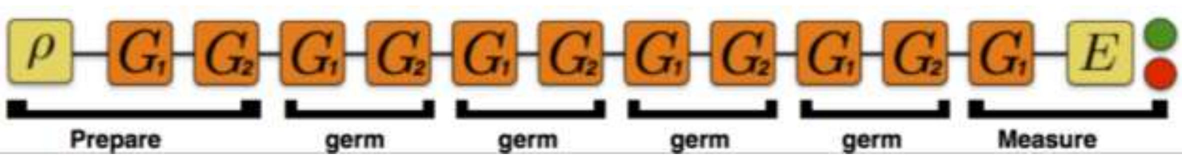

Single qubit gates

Microwave gates

Raw data poor gates

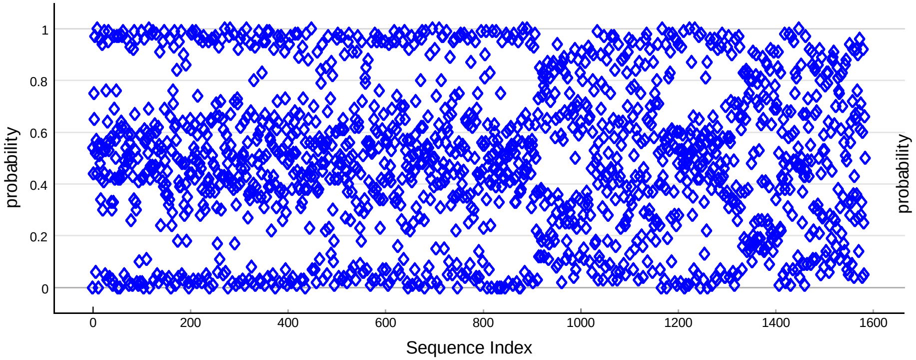

Raw data good gates

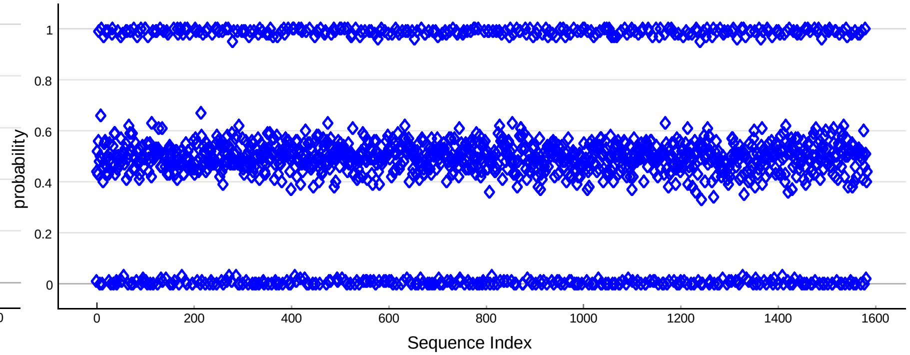

Gate	Rotn. axis	Angle
G_I	0.5252 -0.009 0.8506 -0.0244	0.001699π
G_X	-3×10^{-6} -1 -3×10^{-5} -0.009	0.501308π
G_Y	-0.2474 0.0001 0.9689 -0.0001	0.501366π

Gate	Rotn. axis	Angle
G_I	-0.0035 0.014 -0.9999 0.0006	0.001769π
G_X	-3×10^{-5} -1 1×10^{-4} 0.0006	0.500007π
G_Y	0.1104 4×10^{-5} 0.9939 0.0005	0.50001π

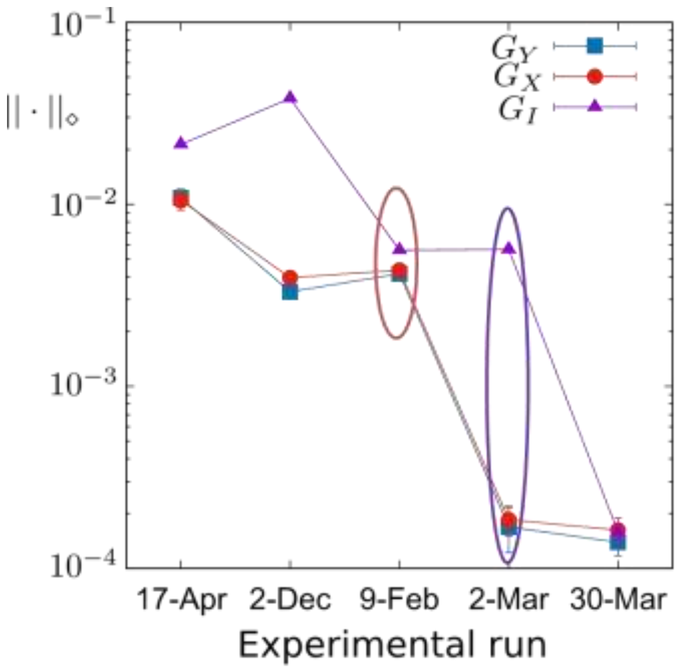

Single qubit gates
Markovianity violation

- BB1 decoupled microwave gates with decoupled identity have very small non-Markovian noise
- BB1 dynamically compensated pulse sequences
- Decoupling sequence for identity gate
- Drift control for π-time and qubit frequency

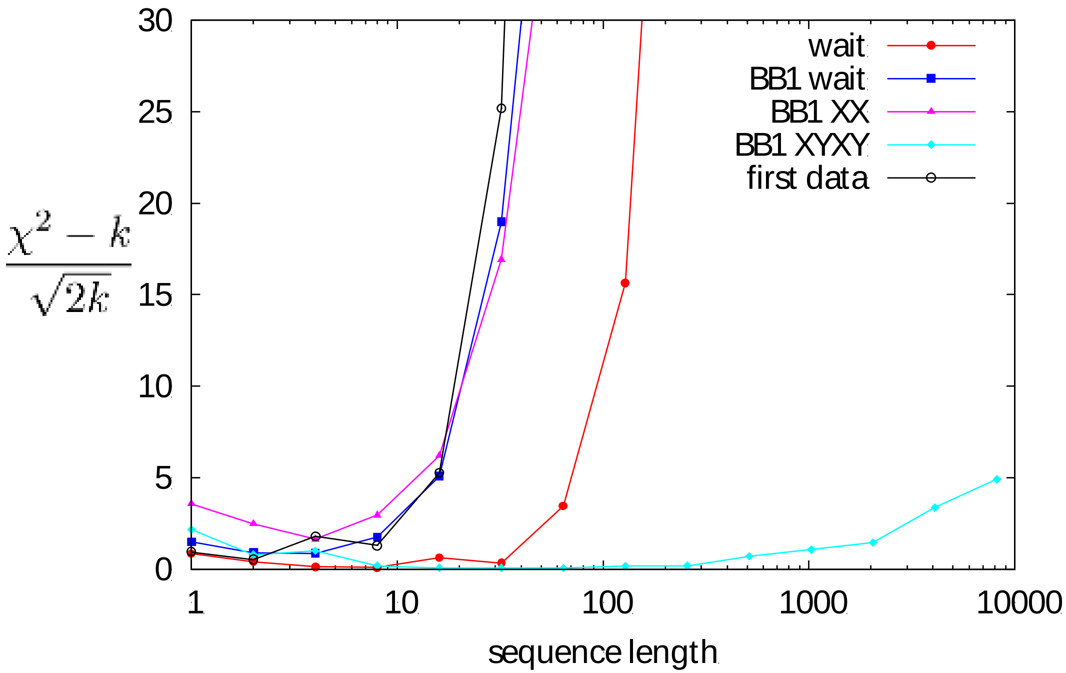

Gate	Process Infidelity	1/2 ◇-Norm
G_I	$6.9(6) \times 10^{-5}$	$7.9(7) \times 10^{-5}$
G_X	$6.1(7) \times 10^{-5}$	$7.0(15) \times 10^{-5}$
G_Y	$7.2(7) \times 10^{-5}$	$8.1(15) \times 10^{-5}$

95% confidence intervals

R. Blume-Kohout, et al. arXiv:1605.07674 (2016)

Microwave broadband pulses

BB1 compensated pulse

Switching artifacts

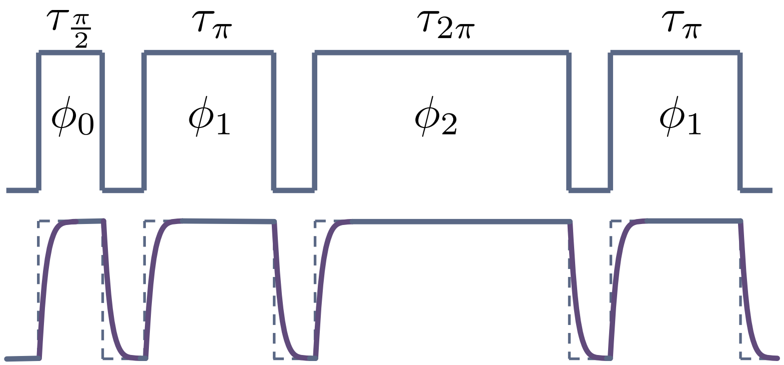

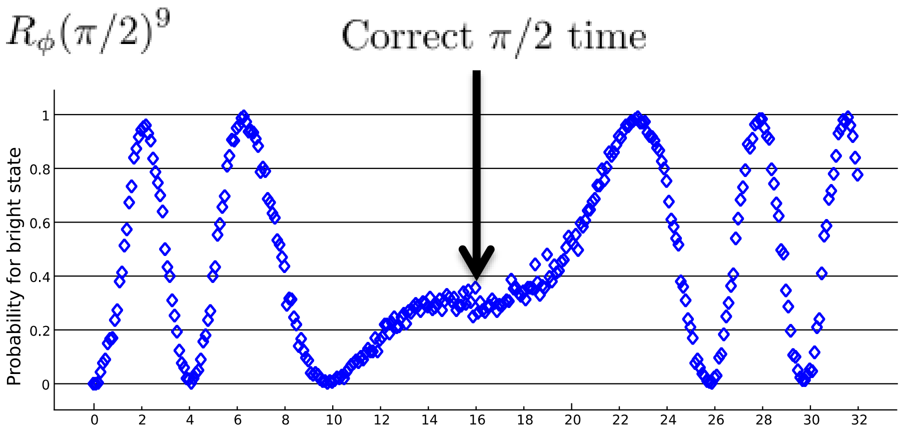

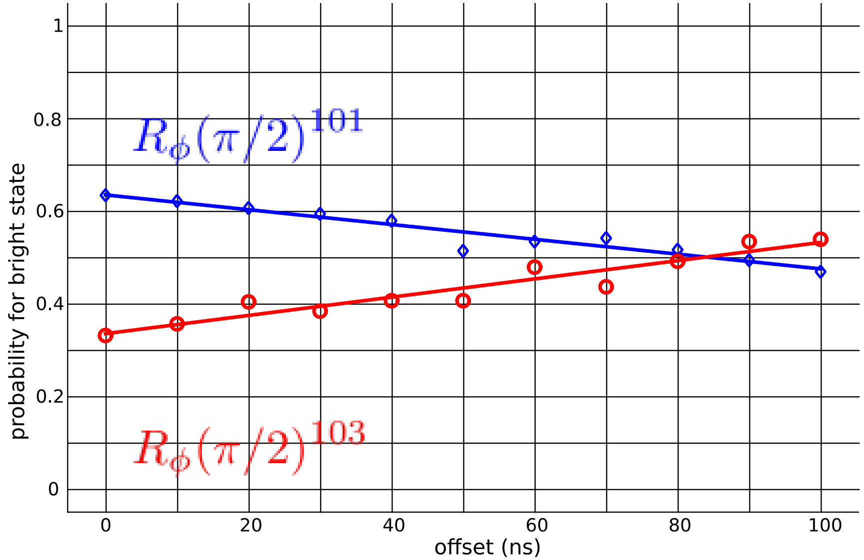

Discontinuous phase updates are used in place of gaps. Solves issues related to finite turn-on time and allows for continuous feedback on the driving field power.

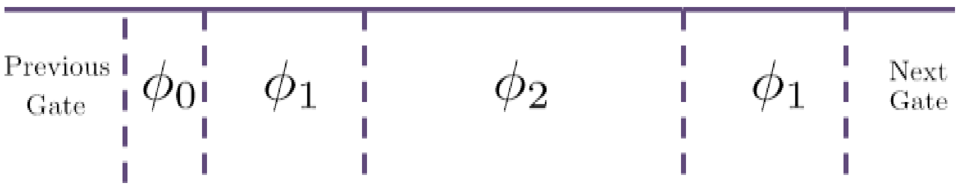

Single qubit gates

Microwave error sources

- Time resolution:
  - Current time resolution is 5 ns
  - π-times are 45 μs
  - ratio: 10^{-4}
  - Possible due to broadband pulses
- Coherence time:
  - $T_2^* = 1\,\mathrm{s}$
  - longest pulse sequences 8192 : 1.66 s

Laser based Raman gates

co-propagating beam geometry
- Motion independent
- No optical phase imprinted

- BB1 dynamically compensated pulse sequences

GST results:

95% confidence intervals

	Conventional pulses		Gapless pulses	
Gate	Process Infidelity	$\frac{1}{2}$ $\diamond$-Norm	Process Infidelity	$\frac{1}{2}$ $\diamond$-Norm
G_I	$0.05(2) \times 10^{-4}$	$12(1) \times 10^{-4}$	$1.1(1) \times 10^{-4}$	$5.3(2) \times 10^{-4}$
G_X	$1.3(1) \times 10^{-4}$	$4(2) \times 10^{-4}$	$0.5(1) \times 10^{-4}$	$2(6) \times 10^{-4}$
G_Y	$1.6(4) \times 10^{-4}$	$4(3) \times 10^{-4}$	$0.7(1) \times 10^{-4}$	$4(9) \times 10^{-4}$

$$\text{Process Infidelity} < 1.2 \times 10^{-4}$$
$$\tfrac{1}{2}\diamond\text{-Norm} < 5.5 \times 10^{-4}$$

Two qubit gates

Mølmer-Sørensen gates

- Mølmer-Sørensen gates [1]
- All two-qubit gates implemented using Walsh compensation pulses [2]

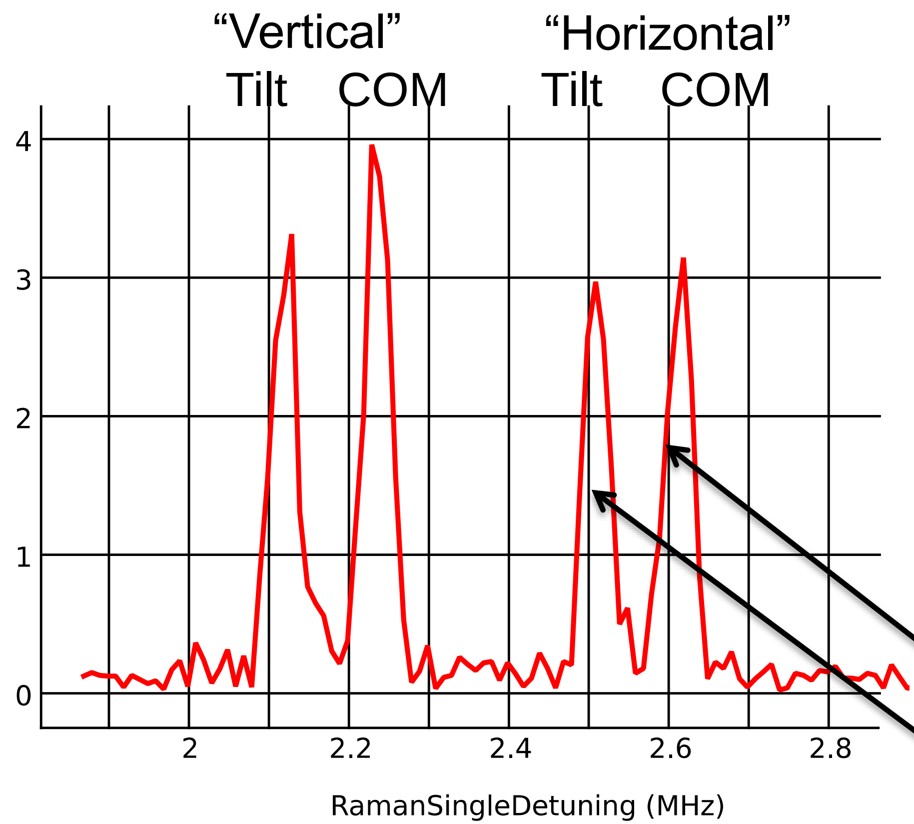

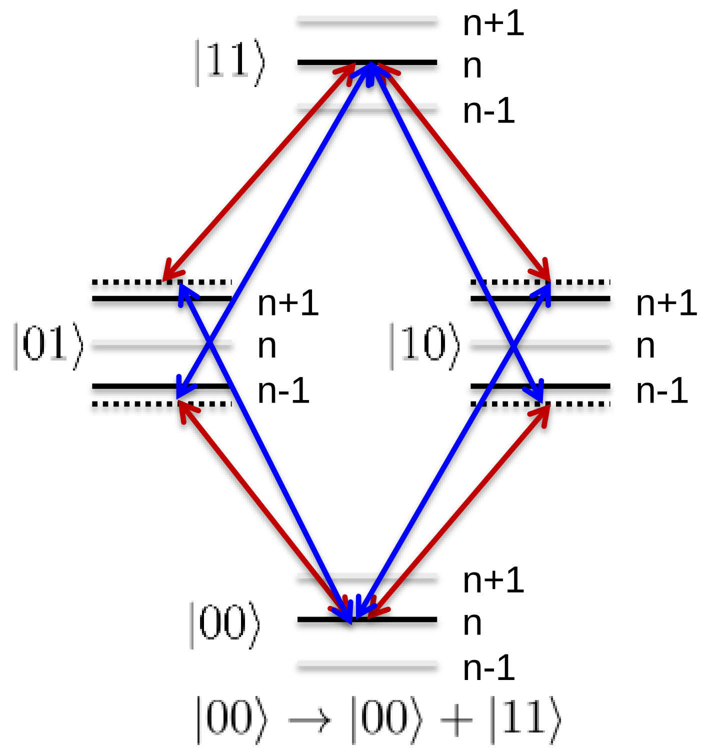

Heating rates

$\approx 60\ \mathrm{quanta}/\mathrm{s}$

$< 8\ \mathrm{quanta}/\mathrm{s}$

[1] K. Mølmer, A. Sørensen, PRL 82, 1835 (1999)
[2] D. Hayes et al. Phys. Rev. Lett. 109, 020503 (2012)

Two qubit gates

Fidelity measurement using parity scan

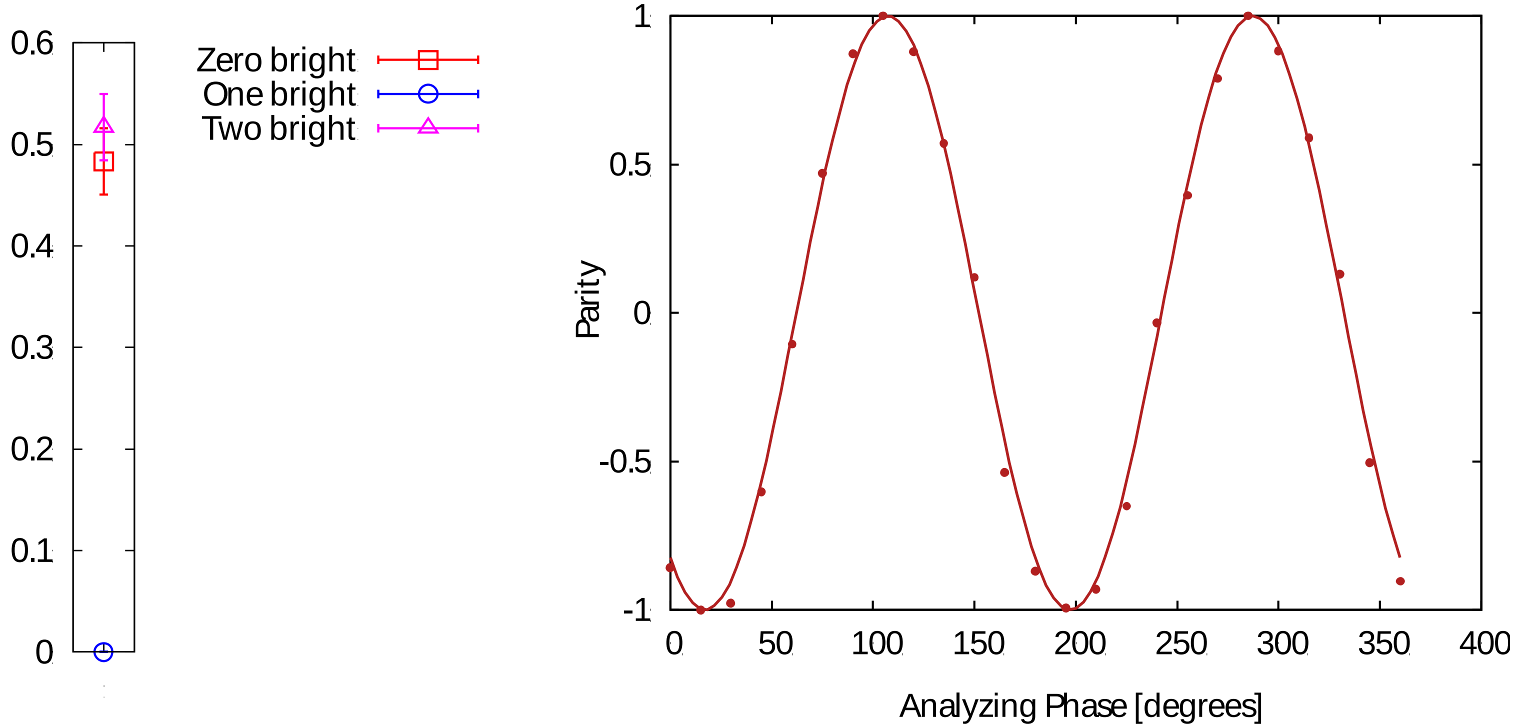

$$\mathcal{F} = \frac{1}{2}(P(|00\rangle) + P(|11\rangle)) + \frac{1}{4}c \approx 0.995$$

Two qubit gates
GST on symmetric subspace

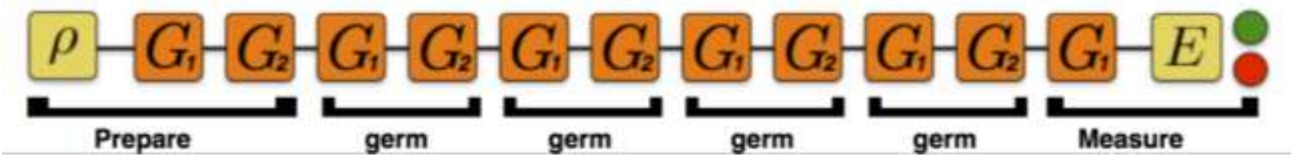

Basic gates: G_I

$$G_{XX} = G_X \otimes G_X$$

$$G_{YY} = G_Y \otimes G_Y$$

$$G_{MS}$$

Preparation Fiducials:

$\{\}$

G_{XX}

G_{YY}

G_{MS}

$G_{XX}G_{MS}$

$G_{YY}G_{MS}$

Germs:

G_I

G_{XX}

G_{YY}

G_{MS}

$G_I G_{XX}$

$G_I G_{YY}$

$G_I G_{MS}$

$G_{XX}G_{YY}$

$G_{XX}G_{MS}$

$G_{YY}G_{MS}$

$G_I G_I G_{XX}$

$G_I G_I G_{YY}$

Detection Fiducials:

$\{\}$

G_{XX}

G_{YY}

G_{MS}

$G_{XX}G_{MS}$

$G_{YY}G_{MS}$

G_{XX}^3

G_{YY}^3

$G_{YY}^2 G_{MS}$

Two qubit gates
GST data

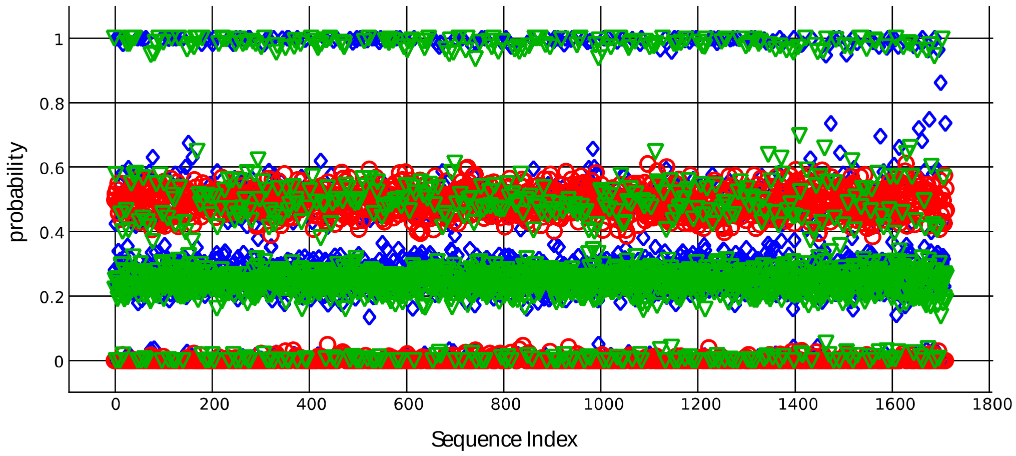

Zero ions bright
One ion bright
Two ions bright

Gate	Process infidelity	$\frac{1}{2}$ Diamond norm
G_I	$1.6 \times 10^{-3} \pm 1.6 \times 10^{-3}$	$28 \times 10^{-3} \pm 7 \times 10^{-3}$
G_{XX}	$0.4 \times 10^{-3} \pm 1.0 \times 10^{-3}$	$27 \times 10^{-3} \pm 5 \times 10^{-3}$
G_{YY}	$0.1 \times 10^{-3} \pm 0.9 \times 10^{-3}$	$26 \times 10^{-3} \pm 4 \times 10^{-3}$
G_{MS}	$4.2 \times 10^{-3} \pm 0.6 \times 10^{-3}$	$38 \times 10^{-3} \pm 5 \times 10^{-3}$

95% confidence intervals

Process fidelity of two-qubit Mølmer-Sørensen gate > 99.5%

Acknowledgments

R. Blume-Kohout, M. G. Blain, C. Clark, S. Clark, K. Fortier, R. Haltli, E. Heller, C. Hogle, A. Hollowell, D. Lobser, P. Maunz, J. Mizrahi, E. Nielsen, P. Resnick, J. Rembetski, K. Rudinger, J. D. Sterk, C. Tigges, J. Van Der Wall